https://www.cytojournal.com/

CytoJournal

Editor-in-Chief:
Miaoqing Zhao, PhD., MD (Shandong First Medical University, Jinan, China)
He Wang, MD, PhD (Yale University School of Medicine, New Haven, Connecticut, USA)
Founding Editor & Editor-in-chief Emeritus:
Vinod B. Shidham, MD, FIAC, FRCPath (WSU School of Medicine, Detroit, USA)

OPEN ACCESS

Research Article

E2F1-mediated *ESPL1* transcriptional activation predicts poor prognosis and promotes the proliferation of leiomyosarcoma

Xiaojuan Yang, BS[1], Guihua Miao, MS[1], Qin Wang, MS[1], Qin Yu, BS[1], Qinsheng Hu, MD[2], Gang Tan, MD[3]

[1]Department of Orthopedic Surgery, West China Hospital, Sichuan University/West China School of Nursing, [2]Department of Orthopedic Surgery, Ya'an People's Hospital, Ya'an, Sichuan, [3]Department of Orthopedics, West China School of Public Health and West China Fourth Hospital, Sichuan University, Chengdu, China.

***Corresponding author:**

Gang Tan,
Department of Orthopedics, West China School of Public Health and West China Fourth Hospital, Sichuan University, Chengdu, Sichuan, China.

gangzhao473028@163.com

Received: 04 September 2024
Accepted: 06 December 2024
Published: 08 January 2025

DOI
10.25259/Cytojournal_178_2024

Quick Response Code:

Supplementary material available at:
https:dx.doi.org/10.25259/Cytojournal_178_2024

ABSTRACT

Objective: Soft tissue and bone cancers, collectively known as sarcomas, constitute a diverse array of uncommon tumors originating from connective tissues. Among sarcomas, leiomyosarcoma (LMS) is one of the most frequently encountered subtypes. This study aims to investigate the expression, clinical significance, biological regulation, and dysregulation mechanisms of extra spindle pole bodies like 1 (*ESPL1*), a gene critical for cell cycle regulation in LMS.

Material and Methods: Bioinformatics analysis was performed using the data from The Cancer Genome Atlas-Sarcoma and Genotype-Tissue Expression datasets. Functional experiments to assess cell proliferation and the cell cycle were performed in LMS cells (SK-LMS-1) after *ESPL1* knockdown. Bioinformatics analyses were conducted to identify the potential transcriptional regulators of ESPL1. The regulatory relationship between *ESPL1* and the E2F transcription factor 1 (E2F1) was validated through the various molecular assays.

Results: *ESPL1* is significantly overexpressed in LMS compared with normal muscle tissue. High *ESPL1* expression is associated with a shorter progression-free interval (PFI) in sarcoma patients, particularly in the LMS subset. *ESPL1* expression might be an independent prognostic factor for poor overall survival and PFI in LMS patients. Functional studies in the LMS cell line SK-LMS-1 demonstrated that *ESPL1* knockdown slowed cell proliferation and increased G2/M cell cycle arrest, suggesting its crucial role in maintaining LMS cell viability and genomic integrity. Further bioinformatics analysis identified the E2F1 transcription factor as a key regulator of ESPL1 expression in LMS. Mechanistic investigations demonstrated that E2F1 interacts with the *ESPL1* promoter, leading to transcriptional activation.

Conclusion: These findings highlight the ESPL1-E2F1 axis as a potential prognostic biomarker and therapeutic target in LMS.

Keywords: Leiomyosarcoma, Extra spindle pole bodies like 1, E2F1, Cell cycle, Proliferation

INTRODUCTION

Sarcomas are a group of rare mesenchymal malignancies that originate from various connective tissues, including bone, cartilage, muscle, fat, blood vessels, and fibrous tissue.[1] Leiomyosarcoma (LMS) is the most common subtype of soft-tissue sarcoma, accounting for 10–20% of all soft-tissue sarcoma cases.[2] LMS arises from smooth muscle cells and can occur in various

anatomical locations, such as the uterus, retroperitoneum, extremities, and visceral organs.[3] Owing to its aggressive clinical behavior and resistance to conventional therapies, the prognosis for patients with advanced or metastatic LMS remains poor.[3]

Elucidating the molecular mechanisms underlying LMS pathogenesis is crucial for the development of novel targeted therapies.[4] Previous studies have identified complex genetic and epigenetic alterations in LMS, such as genetic losses in regions encoding phosphatase and tensin homolog (PTEN) (10q11–21.2), RB transcriptional corepressor 1 (RB1) (13q14.3–q21.1), and TP53 (17p13); inactivating mutations and deletions in TP53 and RB1; PTEN inactivation; and aberrations in the RB1, cyclin D1 (CCND1), cyclin D3 (CCND3), and cyclin-dependent kinase inhibitor 2A (CDKN2A) pathways.[3,5] These proteins are involved in controlling proliferation signaling and the progression of the cell cycle. To maintain the viability of LMS cells, disrupting cell cycle checkpoint regulation through pathways involving RB1, CDKN2A/B, MYC proto-oncogene, bHLH transcription factor (MYC), F-box and WD repeat domain containing 7 (FBXW7), or NF1 is essential.[5]

ESPL1 (extra spindle pole bodies like 1, encoded by the *ESPL1* gene) is a separase that regulates sister chromatid separation during mitosis and meiosis.[6] Although the function of ESPL1 in cell cycle regulation is well documented,[7,8] its involvement in cancer, particularly sarcomas, is not fully understood. Previous studies have indicated that aberrant expression of cell cycle regulators, including those involved in chromatid cohesion and separation, can contribute to LMS tumorigenesis and tumor progression by promoting genomic instability.[5] Its expression can be activated by c-MYB in BCR-ABL-positive chronic myeloid leukemia[9] and by PAX2 in bladder cancer[10] through promoter binding.

In this study, we aim to investigate the expression, clinical significance, biological regulation, and dysregulation mechanisms of *ESPL1*, a gene critical for cell cycle regulation in LMS.

MATERIAL AND METHODS

Datasets and bioinformatics analysis

The Cancer Genome Atlas-Sarcoma (TCGA-SARC) dataset was acquired using the University of California, Santa Cruz (UCSC) Xena Browser (https://xena.ucsc.edu/).[11] The dataset includes various subtypes of sarcoma: LMS, dedifferentiated liposarcoma (DDLPS), myxofibrosarcoma (MFS), malignant peripheral nerve sheath tumors (MPNST), synovial sarcoma (SS), and undifferentiated pleomorphic sarcoma (UPS). Normal muscle tissue gene expression data were obtained from the genotype-tissue expression (GTEx) project. A total of 396 normal muscle samples were used for comparison with LMS tissues in the TCGA-SARC dataset. The Z scores of 1387 constituent PAthway Representation and Analysis by Direct Reference on Graphical Models (PARADIGM) pathways in LMS patients in the TCGA-SARC cohort were also obtained using the UCSC Xena browser. The correlation between *ESPL1* expression and the activity of each pathway was estimated by calculating Pearson's correlation coefficient. Only pathways with Pearson's $r > 0.80$ were considered for further analysis.

The transcript expression data of *ESPL1* during different cell cycle phases were obtained from the Human Protein Atlas (HPA) database (https://www.proteinatlas.org/),[12] specifically for the U-2 OS cell line.

The Cistrome Data Browser (http://cistrome.org/db/), a comprehensive database for regulatory genomics[13] was used to identify the chromatin regulators and transcription factors potentially binding to the *ESPL1* promoter (HPRM47346; from Genecopoeia) within 1 kb of the transcription start site (TSS). The correlation between *ESPL1* expression and the expression of the identified chromatin regulators and transcription factors was assessed in primary LMS samples from the TCGA-SARC. Significant correlations (Pearson's $r > 0.50$) were considered for further analysis.

Kaplan-Meier survival analyses

Kaplan-Meier survival curves were generated for progression-free interval (PFI) and overall survival (OS) in the entire sarcoma cohort and the LMS subset. Patients with primary tumors were grouped based on the median expression of *ESPL1*.

Immunohistochemistry (IHC) analysis

IHC images of ESPL1 in normal smooth muscle tissue were obtained from the HPA database.[12] Commercial tissue microarrays containing LMS tissues were obtained from Bioaitech (Xi'an, China) and used to examine ESPL1 protein expression with a BOND-III Automated IHC/ISH Stainer (Leica Biosystems, Germany). The tissue sections were first deparaffinized, rehydrated, and subjected to antigen retrieval using BOND Epitope Retrieval Solution 1 (Leica Biosystems). Primary antibodies specific to ESPL1 (LS-B8366; LSBio, Shirley, MA, USA) were applied, and visualization was achieved using the BOND Polymer Refine Detection system (DS9800-CN; Leica Biosystems, Germany) and a real-time digital pathology system (Aperio LV1; Leica Biosystems).

Cell culture and transfection

Human LMS representative SK-LMS-1 cells (HTB-88) were obtained from the American Type Culture Collection (Manassas, VA, USA) and were cultured as recommended.

We performed short tandem repeat (STR) identification and confirmed that the STR profile of this cell line matched the records in the database, confirming its identity. In addition, we conducted mycoplasma testing, and the results indicated that the cell line was free of mycoplasma contamination. The cells were transfected with small interfering RNAs (50 nM) targeting *ESPL1* (siESPL1#1, #2, #3), E2F1 (siE2F1#1, #2, #3) or nontargeting control siRNA (siNC) using Lipofectamine RNAiMAX (Thermo Fisher Scientific, USA).

Quantitative real-time polymerase chain reaction (qRT-PCR)

Total RNA was extracted from transfected SK-LMS-1 cells using the RNeasy Plus Mini Kit (74134; Qiagen, Germany) and reverse-transcribed into cDNA using the High-Capacity cDNA Reverse Transcription Kit (4368814; Applied Biosystems, USA). *ESPL1* and *E2F1* mRNA levels were quantified by qRT-PCR using SYBR Green Master Mix (Applied Biosystems) on a QuantStudio 3 Real-Time PCR System (Applied Biosystems). The following primers were used: *ESPL1*, forward sequence, 5'-ATCTCTGTCAGTCGGACCTGCA-3'; reverse sequence, 5'-CAGGTGGACCTTCTTCACAGAG-3'; *E2F1*, forward sequence, 5'- GGACCTGGAAACTGACCATCAG-3'; reverse sequence, 5'- CAGTGAGGTCTCATAGCGTGAC-3'; *GAPDH* (as an internal reference), forward sequence, 5'- GTCTCCTCTGACTTCAACAGCG-3'; reverse sequence, 5'- ACCACCCTGTTGCTGTAGCCAA-3'. Relative expression levels were calculated using the $2^{-\Delta\Delta Ct}$ method.

Western blotting

Total protein was extracted from transfected SK-LMS-1 cells using radioimmunoprecipitation assay (RIPA) buffer supplemented with protease inhibitors (P0013; Beyotime, China). The protein concentration was determined using the bicinchoninic acid (BCA) protein assay kit (P0010; Beyotime). Protein lysates were separated by sodium dodecyl sulfate polyacrylamide gel electrophores (SDS-PAGE) (30 μg/lane) and transferred to polyvinylidene fluoride (PVDF) membranes (FFP39; Beyotime). The membranes were blocked with 5% nonfat milk in Tris Buffered Saline with Tween 20 (TBST) for 1 h at room temperature and then probed overnight at 4°C with primary antibodies specific to ESPL1 (1:1000; LS-B8366; LSBio), E2F1 (1:1000; 3742; Cell Signaling Technology), and β-actin (1:20000; 66009-1-Ig; Procell). After being washed 3 times with TBST for 10 min each, the membranes were incubated with an HRP-conjugated secondary antibody (1:5000; SA00001-2; Proteintech, China) for 1 h at room temperature. The protein bands were visualized using an ECL substrate (32209; Thermo Fisher Scientific) and detected using a chemiluminescent imaging system (Tanon 5200; Tanon Science and Technology, China). Densitometric analysis was performed using ImageJ software (NIH, USA), with β-actin serving as the loading control.

Cell growth assessment

The cell counting kit-8 (CCK-8) assay (CK04; Dojindo, Japan) was used to evaluate cell viability at 0, 24, 48, and 72 h posttransfection. The absorbance at 450 nm was measured using a microplate reader (BioTek Epoch, Agilent Technology, USA). Transfected SK-LMS-1 cells were seeded into 12-well plates and cultured for 10–14 days. Colonies were fixed with methanol, stained with 0.5% crystal violet for 30 min, and counted. The colony formation efficiency was normalized to that of the control group.

Flow cytometry analysis of the cell cycle distribution

SK-LMS-1 cells were fixed in ice-cold ethanol, stained with propidium iodide (PI) solution containing RNase A (#4087; Cell Signaling Technology, USA), and analyzed using a BD Accuri C6 flow cytometer. The cell cycle phases were quantified using NovoExpress (v.1.5.2; Agilent Technology).

Chromatin immunoprecipitation (ChIP) and qPCR

The ChIP assay was performed using the SimpleChIP Enzymatic Chromatin IP Kit (#9002; Cell Signaling Technology, USA). SK-LMS-1 cells were fixed with formaldehyde to cross-link proteins to DNA, lysed, and sonicated to shear the DNA into 200–1000 bp fragments. Chromatin fragments were immunoprecipitated with antibodies against E2F1 or normal IgG as a control. The DNA-protein complexes were reversed, and the DNA was purified. Precipitated DNA was analyzed by qPCR using primers specifically designed for the E2F1-binding region in the ESPL1 promoter (24–125 bp), with the following primers: Forward, 5'-GTACTGGTCAGGCGGTTAAG-3' and reverse, 5'-TTCACTTCAGCACGTACCC-3.' qPCR was then performed as described above. The results are expressed as % input normalized to the amount of input chromatin.

Dual-luciferase reporter assay

The full *ESPL1* promoter region (−1402 to +213) and a truncated promoter region (−100 to +213) were chemically synthesized, cloned, and inserted into the pGL3-basic vector (E1751; Promega, Germany) upstream of the firefly luciferase gene. SK-LMS-1 cells were cotransfected with siNC or siE2F1 (#2) and the pGL3 constructs using Lipofectamine 3000 (Thermo Fisher Scientific). At 24 h posttransfection, luciferase activity was measured using the Dual-Luciferase Reporter Assay System (E1910; Promega).

Statistical analysis

All statistical analyses were performed using GraphPad Prism 10.1.2. The log-rank test was used to assess the differences in survival between the groups with high and low *ESPL1* expression. A receiver operating characteristic (ROC) curve was generated to assess the diagnostic value of *ESPL1* expression for differentiating between normal muscle tissues and primary LMS. For comparisons involving multiple groups, a one-way analysis of variance followed by Tukeycee *post hoc* test was applied, whereas unpaired t tests were used for the comparisons between the two groups. The significance threshold was set to $P < 0.05$.

RESULTS

ESPL1 expression and prognostic significance in sarcomas and LMS

ESPL1 expression across different sarcoma subtypes was analyzed in the TCGA-SARC dataset. A significant difference was observed only between the DDLPS and UPS groups ($P = 0.014$) [Figure 1a]. A total of 259 primary sarcoma patients with survival data and 104 LMS patients were included in the survival analysis. K-M survival analysis revealed that higher *ESPL1* expression ($n = 129$; top 50%) was significantly associated with worse PFI [Figure 1b; $P = 0.003$] and OS [Figure 1c; $P = 0.02$] than lower *ESPL1* expression (bottom 50%) in the entire TCGA-SARC cohort.

Since we focused on LMS, we compared *ESPL1* expression in the LMS subset with that in normal muscle tissues via GTEx. *ESPL1* was significantly overexpressed in LMS tissues ($n = 104$) compared with normal muscle tissues (GTEx-NS, $n = 396$) ($P < 0.001$) [Figure 1d]. To assess the diagnostic value of *ESPL1* expression in distinguishing between normal muscle tissues and LMS, ROC curve analysis was performed. The ROC curve demonstrated high diagnostic accuracy, with an AUC of 0.993 [Figure 1e]. Survival analysis revealed that higher *ESPL1* expression in the LMS subset was significantly correlated with a worse PFI [Figure 1f, $P < 0.001$) and OS in the LMS subset [Figure 1g, $P = 0.043$].

To validate ESPL1 expression at the protein level, we retrieved IHC staining data for ESPL1 in normal smooth muscle tissue from the HPA database and performed IHC analysis on a commercial tissue microarray of LMS tissues. The results confirmed positive ESPL1 staining in LMS tissues, whereas minimal ESPL1 staining was detected in normal smooth muscle tissues [Figure 1h].

We next sought to assess whether ESPL1 expression serves as an independent prognostic biomarker in LMS. The key clinicopathological parameters of LMS patients with high and low *ESPL1* expression are compared in Table 1. No significant differences were observed in OS status ($P = 0.160$) or age at initial pathologic diagnosis ($P = 0.597$) between the two groups. However, the PFI status was significantly different, with a greater proportion of patients with high *ESPL1* expression experiencing disease progression (36.5% vs. 20.2%, $P < 0.001$). The sex distribution was similar between the two groups ($P = 0.676$). With respect to residual tumor status, a greater percentage of patients with high *ESPL1* expression had R0 resection (34.6% vs. 33.7%, $P = 0.077$). In addition, margin status did not differ significantly between the groups ($P = 0.206$), with a slightly greater proportion of negative margins in the high-*ESPL1* subgroup (41.5% vs. 31.7%) [Table 1].

We subsequently conducted univariate and multivariate analyses for OS [Table 2] and PFI [Table 3] in patients with LMS. According to the univariate analysis, high *ESPL1* expression was associated with poorer OS (Hazard ratio [HR] = 1.467; 95% confidence interval [CI]: 1.102–1.952; $P = 0.009$). High *ESPL1* expression remained an independent prognostic factor for poor OS (HR = 1.837; 95% CI: 1.249–2.704; $P = 0.002$) after adjustment for margin status in the multivariate analysis [Table 2].

According to the univariate analysis, higher *ESPL1* expression was associated with a significantly shorter PFI (HR = 1.543; 95% CI: 1.236–1.925; $P < 0.001$). This relationship remained strong in the multivariate analysis, where *ESPL1* expression independently predicted a worse PFI (HR = 1.683; 95% CI: 1.270–2.231; $P < 0.001$) [Table 3]. Patients with R2 residual tumors had a significantly worse PFI (HR = 4.996; 95% CI: 1.764–14.155; $P = 0.002$). However, in the multivariate analysis, the effect of residual tumor status was no longer significant (HR = 3.752; 95% CI: 0.651–21.615; $P = 0.139$) [Table 3].

Knockdown of *ESPL1* induces G2/M arrest in SK-LMS-1 cells

To explore the molecular mechanisms associated with ESPL1 in LMS, we analyzed the correlation between *ESPL1* expression and the activity of 1387 constituent PARADIGM pathways in LMS cases from the TCGA-SARC dataset [Supplementary Table 1]. The heatmap [Figure 2a] shows the most significant correlations (Pearson's r > 0.80) between *ESPL1* expression and biological pathways. Higher *ESPL1* expression levels were associated with increased activity in pathways such as the following: Mitotic_prometaphase; kinesins; E2F_transcription_factor_network; resolution_of_Sister_Chromatid_cohesion; Aurora_B_signaling; PLK1_signaling_events; FOXM1_transcription_factor_network; E2F_mediated_regulation_of_DNA_replication; G1/S-Specific_Transcription; mitotic_metaphase/anaphase_transition; and separation_of_Sister_chromatids [Figure 2a]. These pathways are generally related to mitotic processes, transcription factor networks, and chromatid

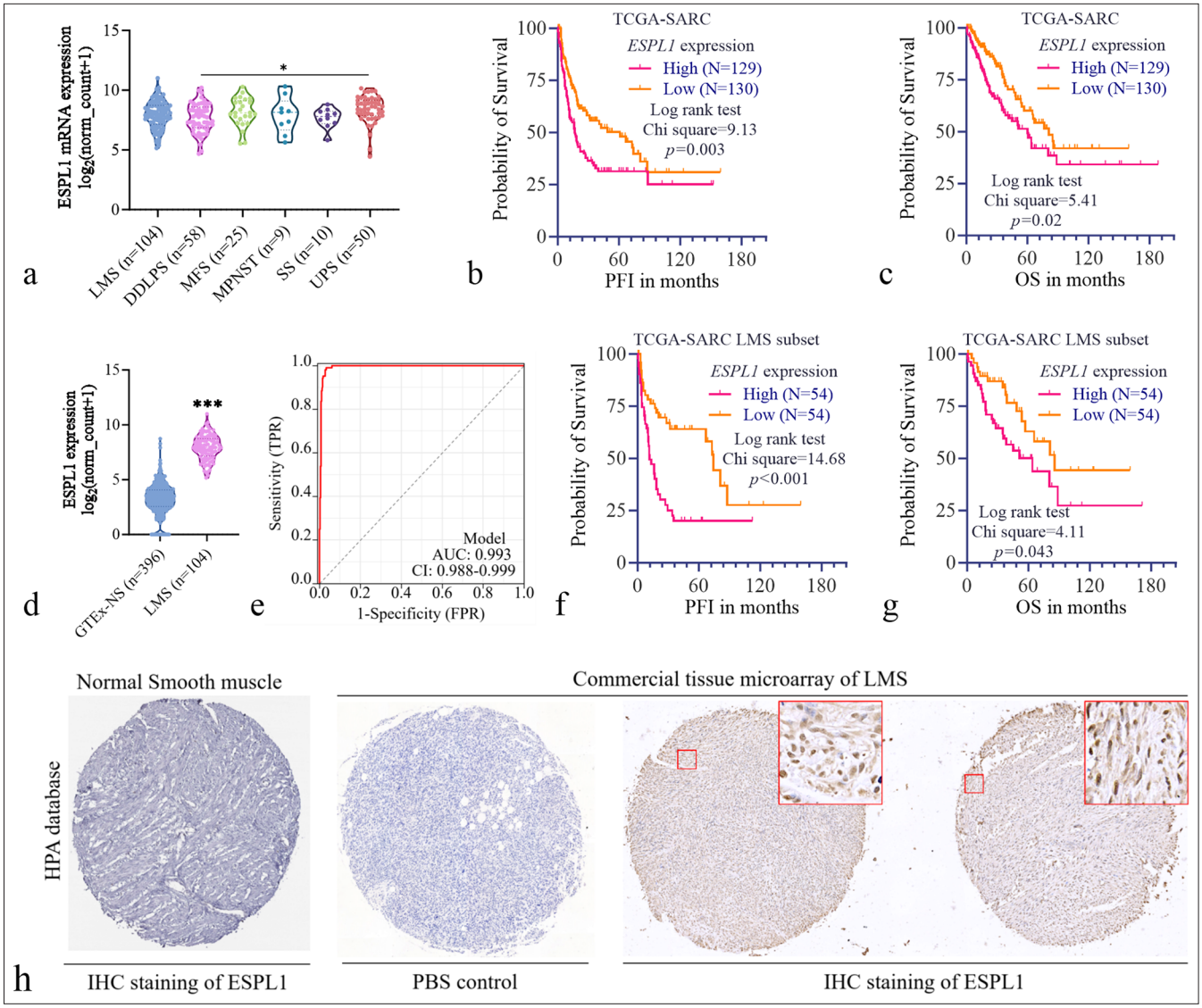

Figure 1: *ESPL1* expression and prognostic significance in sarcomas and leiomyosarcoma. (a) Violin plot showing *ESPL1* expression across different sarcoma subtypes in the TCGA-SARC dataset. (b and c) Survival analysis for PFI (b) and OS (c) in primary sarcomas in the TCGA-SARC cohort. Patients were grouped by high (orange) or low (pink) *ESPL1* expression. The median *ESPL1* expression level was set as the cutoff. (d) Violin plot comparing *ESPL1* expression between normal muscle tissues from the GTEx dataset (GTEx-NS, *n*=396) and primary LMS tissues from the TCGA-SARC cohort (*n*=104). (e) ROC curve illustrating the diagnostic value of *ESPL1* expression for differentiating between normal muscle tissues and primary LMS tissues using the expression data in panel (d). (f and g) Survival analysis for PFI (f) and OS (g) in patients with primary LMS in the TCGA-SARC cohort. Patients were grouped by high (orange) or low (pink) *ESPL1* expression. The median *ESPL1* expression level was set as the cutoff. (h) Immunohistochemistry (IHC) analysis of ESPL1 protein expression. IHC staining of ESPL1 in normal smooth muscle tissue was performed using the HPA database via https://images.proteinatlas.org/73188/166539_B_5_7.jpg. A commercial tissue microarray of LMS tissues showed positive IHC staining for ESPL1 at the protein level. The insets show higher magnification images of the staining patterns. *ESPL1*: Extra spindle pole bodies like 1, TCGA-SARC: The cancer genome atlas sarcoma, GTEx: Genotype-tissue expression, LMS: Leiomyosarcoma, ROC: Receiver operating characteristic, DDLPS: Dedifferentiated liposarcoma; MFS: Myxofibrosarcoma; MPNST: Malignant peripheral nerve sheath tumors; SS: Synovial sarcoma; UPS: Undifferentiated pleomorphic sarcoma; PFI: Progression-free interval; OS: Overall survival; TPR: True positive rate; FPR: False positive rate; PBS: Phosphate buffered saline.

cohesion, suggesting a role for ESPL1 in cell cycle regulation and genomic stability.

The variation in *ESPL1* transcript expression during different phases of the cell cycle was investigated in U-2 OS cells based on subcellular data from the HPA. Box plot analysis [Figure 2b] revealed that *ESPL1* expression varied during the cell cycle, with higher expression observed in the S-tr and S&G2 phases than in the G1 phase. A continuous scatter

plot analysis over a 24-h cell cycle period [Figure 2c] further confirmed that *ESPL1* expression fluctuated, with peak levels occurring in the late S and G2/M phases. To assess the functional impact of *ESPL1* knockdown, LMS representative SK-LMS-1 cells were transfected with siRNAs targeting *ESPL1* (siESPL1#1, #2, #3) or nontargeting control siRNA (siNC). qRT-PCR confirmed the significant decrease in *ESPL1* mRNA levels in the siESPL1 groups compared with the siNC group [Figure 2d]. Western blot analysis further validated the reduction in ESPL1 protein levels 24 h post-transfection [Figure 2e and f].

A cell proliferation assay (CCK-8) demonstrated that *ESPL1* knockdown significantly reduced the viability of SK-LMS-1 cells over a 72-h period [Figure 2g]. Additionally, the colony formation assay revealed a significant decrease in clonogenic capacity upon *ESPL1* knockdown [Figure 2h and i]. To determine how *ESPL1* knockdown influences the cell cycle, we performed flow cytometry analyses of the cell cycle distribution using PI staining. *ESPL1* knockdown resulted in an evident increase in the G2/M population, with a corresponding decrease in the G1 and S phase populations [Figure 2j and k].

Table 1: Key clinicopathological parameters between LMS patients with high and low *ESPL1* expression.

Characteristics	*ESPL1* high (%)	*ESPL1* low (%)	*P*-value
n	52	52	
OS status, *n* (%)			0.160
0	28 (26.9)	35 (33.7)	
1	24 (23.1)	17 (16.3)	
PFI status, *n* (%)			< 0.001
0	14 (13.5)	31 (29.8)	
1	38 (36.5)	21 (20.2)	
Age at initial pathological diagnosis			
Mean ± SD	59.827±12.627	58.615±10.602	0.597
Gender, *n* (%)			0.676
Female	34 (32.7)	36 (34.6)	
Male	18 (17.3)	16 (15.4)	
Residual tumor, *n* (%)			0.077
R0	36 (34.6)	35 (33.7)	
RX	8 (7.7)	3 (2.9)	
R2	3 (2.9)	1 (1)	
R1	5 (4.8)	13 (12.5)	
Margin status, *n* (%)			0.206
Negative	34 (41.5)	26 (31.7)	
Positive	9 (11)	13 (15.9)	

LMS: Leiomyosarcoma, *ESPL1*: Extra spindle pole bodies like 1, OS: Overall survival, PFI: Progression-free interval

Bioinformatics analysis identified E2F1 as a transcription factor with potential regulatory effects on *ESPL1* expression in LMS

To identify potential transcriptional regulators of *ESPL1* in LMS, we conducted a bioinformatics analysis using expression data from the TCGA-SARC dataset. We first identified 200 chromatin regulators and transcription factors that potentially bind to the *ESPL1* promoter [Supplementary Material 1] within 1 kb of the TSS from the Cistrome DB [Supplementary Table 2]. Then, their expression correlation with *ESPL1* in LMS patients in the TCGA-SARC cohort was visualized [Figure 3a] and calculated. Pearson's correlation analysis revealed the top transcription factors and chromatin regulators with potential regulatory effects on *ESPL1* expression, including *RAD51 recombinase*

Table 2: Univariate and multivariate analyses for OS in LMS patients.

Characteristics	Total (*n*)	Univariate analysis		Multivariate analysis	
		Hazard ratio (95% CI)	*P*-value	Hazard ratio (95% CI)	*P*-value
ESPL1 expression	104	1.467 (1.102–1.952)	0.009	1.837 (1.249–2.704)	0.002
Age at initial pathologic diagnosis	104	1.011 (0.983–1.039)	0.447		
Gender	104				
Female	70	Reference			
Male	34	0.802 (0.401–1.603)	0.532		
Margin status	82				
Negative	60	Reference		Reference	
Positive	22	2.331 (1.045–5.203)	0.039	3.170 (1.363–7.370)	0.007

LMS: Leiomyosarcoma, *ESPL1*: Extra spindle pole bodies like 1, OS: Overall survival, CI: Confidence interval

Table 3: Univariate and multivariate analyses of the PFI in LMS patients.

Characteristics	Total (*n*)	Univariate analysis		Multivariate analysis	
		Hazard ratio (95% CI)	*P*-value	Hazard ratio (95% CI)	*P*-value
ESPL1 expression	104	1.543 (1.236–1.925)	<0.001	1.683 (1.270–2.231)	<0.001
Age at initial pathologic diagnosis	104	0.990 (0.968–1.013)	0.391		
Gender	104				
Female	70	Reference			
Male	34	0.863 (0.490–1.520)	0.609		
Residual tumor	104				
R0	71	Reference		Reference	
RX	11	1.364 (0.574–3.241)	0.483	0.798 (0.217–2.932)	0.735
R2	4	4.996 (1.764–14.155)	0.002	3.752 (0.651–21.615)	0.139
R1	18	1.542 (0.786–3.026)	0.208	1.761 (0.641–4.835)	0.272
Margin status	82				
Negative	60	Reference		Reference	
Positive	22	2.084 (1.114–3.900)	0.022	1.770 (0.736–4.252)	0.202

R0: No residual tumor, R1: Microscopic residual tumor, R2: Macroscopic residual tumor, RX: Presence of residual tumor cannot be assessed, CI: Confidence interval

(*RAD51*) (r = 0.71), RAD21 cohesin complex component (*RAD21*) (r = 0.53), *E2F1* (r = 0.49), *TAR DNA binding protein* (*TARDBP*) (r = 0.49) and structural maintenance of chromosomes 1A (*SMC1A*) (r = 0.48) [Figure 3b and c].

While *RAD51* and *RAD21* (two chromatin regulator genes) are strongly correlated with *ESPL1* expression, their roles are more related to DNA repair and homologous recombination than to direct transcriptional regulation.[6,14] *E2F1* is a well-established transcription factor that directly regulates the expression of genes involved in critical cellular processes, including cell cycle progression, DNA damage response, and apoptosis.[15] Given the relevance of these pathways in the pathogenesis of LMS, we focused on E2F1 in this study.

To further validate this potential regulatory relationship, we examined the E2F1 binding motifs (MA0024.2 and MA0024.1) within the *ESPL1* promoter region using the Scan module in JASPAR 2024 [Figure 3d].[16] Only the predicted binding sites with relative scores >0.85 were considered for further analysis [Table 4]. The *ESPL1* promoter region spans chr12: 53266897–53268512, with the TSS at position 53268299. Fourteen potential E2F1 binding sites (green and pink bars) were observed in this region [Figure 3d].

Validation of the effects of E2F1 transcriptional activation on the *ESPL1* promoter in LMS

E2F1 expression was also significantly greater in LMS tissues (TCGA-SARC, *n* = 104) than in normal muscle tissues (GTEx-NS, *n* = 396) [Figure 4a]. Next, we investigated the impact of *E2F1* knockdown on *ESPL1* expression in SK-LMS-1 cells. *ESPL1* expression following transfection with *E2F1* siRNAs was significantly lower than that following transfection with the nontargeting control (siNC) [Figure 4b-f].

To test whether E2F1 directly regulates *ESPL1* promoter activity, we performed a luciferase reporter assay. SK-LMS-1 cells were cotransfected with siNC or siE2F1 (#2) and luciferase reporter constructs based on pGL3-basic containing either the full *ESPL1* promoter region (pGL3/−1402~213) or a truncated promoter region (pGL3/−100~213) [Figure 4g]. The results demonstrated that both pGL3/−1402~213 and pGL3/−100~213 had significantly greater luciferase activity than the pGL3-basic control [Figure 4h]. In addition, *E2F1* knockdown significantly reduced the luciferase activity of these two plasmids but had a limited influence on the activity of the pGL3-basic control [Figure 4h].

To validate the direct binding of E2F1 to the *ESPL1* promoter, we designed a pair of primers covering two predicted E2F1 binding sites in the promoter region (24~125) for ChIP-qPCR analysis [Figure 4g]. ChIP-qPCR analysis was then performed in SK-LMS-1 cells with or without *E2F1* knockdown. The results revealed significant enrichment of E2F1 binding at the *ESPL1* promoter in control cells, which was reduced upon *E2F1* knockdown [Figure 4i].

DISCUSSION

Through bioinformatics analysis of the TCGA-SARC dataset and GTEX, we demonstrated that *ESPL1* is overexpressed in

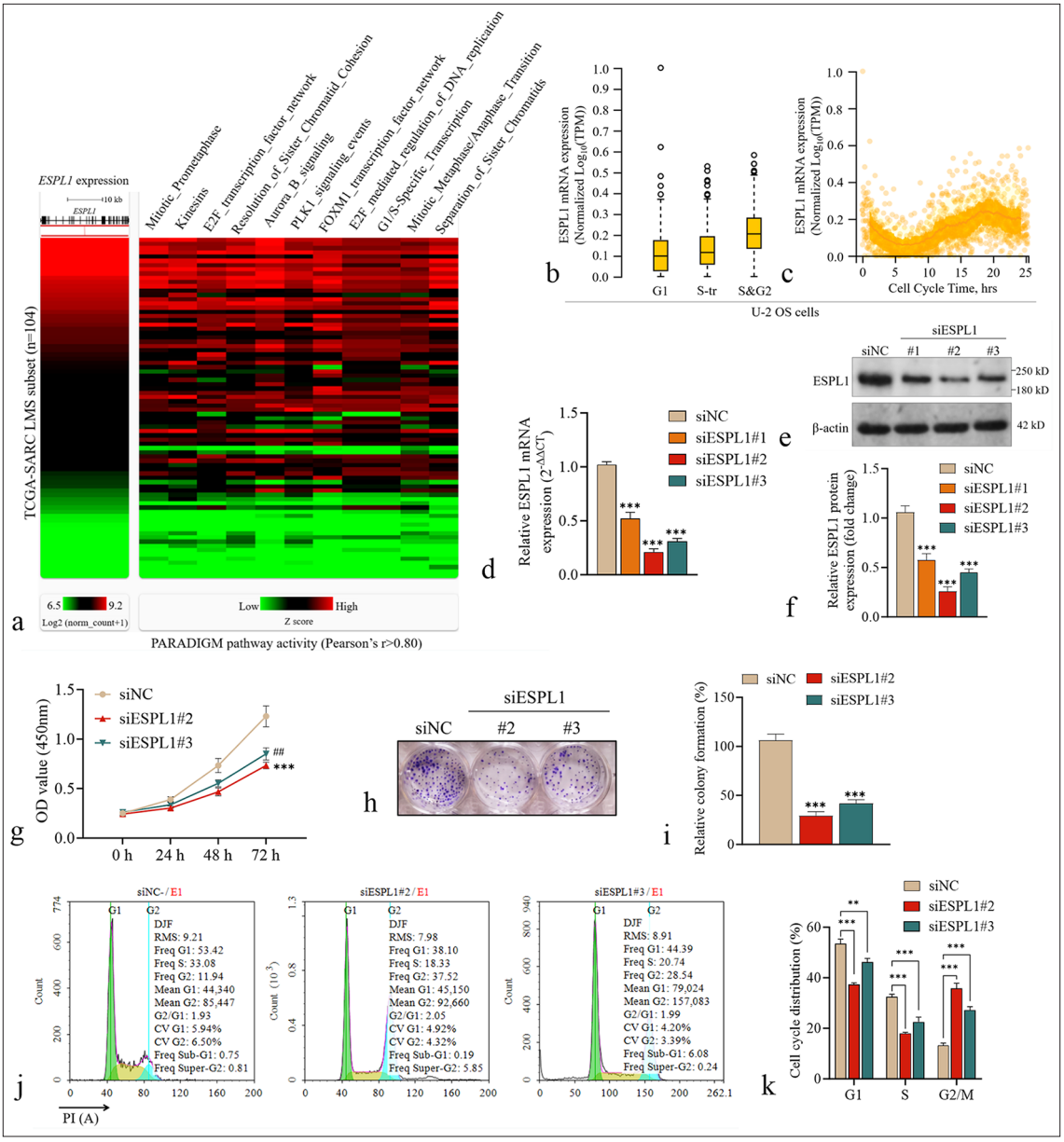

Figure 2: Knockdown of *ESPL1* induces G2/M arrest in SK-LMS-1 cells. (a) Heatmap showing *ESPL1* expression and the activity of constituent PARADIGM pathways in LMS patients from the TCGA-SARC dataset. The rows represent individual LMS cases (n=104), and the columns represent various biological pathways. Pathways with Pearson's r > 0.80 are shown. High expression and pathway activity are indicated in red, whereas low expression and pathway activity are indicated in green. (b) Box plot depicting the variation in normalized *ESPL1* transcript expression (log2[TPM]) during different phases of the cell cycle (G1, S-tr, and S&G2) in U-2 OS cells. Images were obtained from the HPA: https://www.proteinatlas.org/ENSG00000135476-ESPL1/subcellular#cell_cycle. (c) Scatter plot showing the continuous variation in *ESPL1* transcript expression over a 24-h cell cycle period in U-2 OS cells. (d) qRT-PCR validation of *ESPL1* knockdown in SK-LMS-1 cells transfected with siNC or siESPL1 (#1, #2, #3). (e and f) ESPL1 protein levels in SK-LMS-1 cells 24 h after transfection with siNC or siESPL1 (#1, #2, #3). (g) 24 h after the transfection of siNC or siESPL1 (#2, #3), the cell viability at the indicated time points was measured and compared. # indicates a comparison between siESPL1#2 and siNC. * indicates a comparison between siESPL1#3 and siNC. (h and i) Effect of *ESPL1* knockdown on the clonogenic capacity of SK-LMS-1 cells. Representative images (h) of crystal violet-stained colonies and quantification (i) of relative colony formation are shown. (j) Cell cycle distribution of SK-LMS-1 cells transfected with siNC or siESPL1 (#2 and #3). PI staining was used to quantify the cell cycle phases. (k) Quantification of the cell cycle distribution from the flow cytometry data. The data are shown as means ± SD from three independent experiments. ** and $^{\#\#}P$<0.01, ***P<0.001. *ESPL1*: Extra spindle pole bodies like 1, LMS: Leiomyosarcoma, OS: Overall survival, TCGA-SARC: The Cancer Genome atlas sarcoma, qRT-PCR: Quantitative real-time polymerase chain reaction, HPA: Human protein atlas, PLK1: Polo-like kinase 1, FOXM1: Forkhead Box M1, TPM: Transcripts per million., DJF: Doublet-J discriminant function, RMS: Root mean square, si-NC: Small interfering RNA-negative control, OD: Optical density.

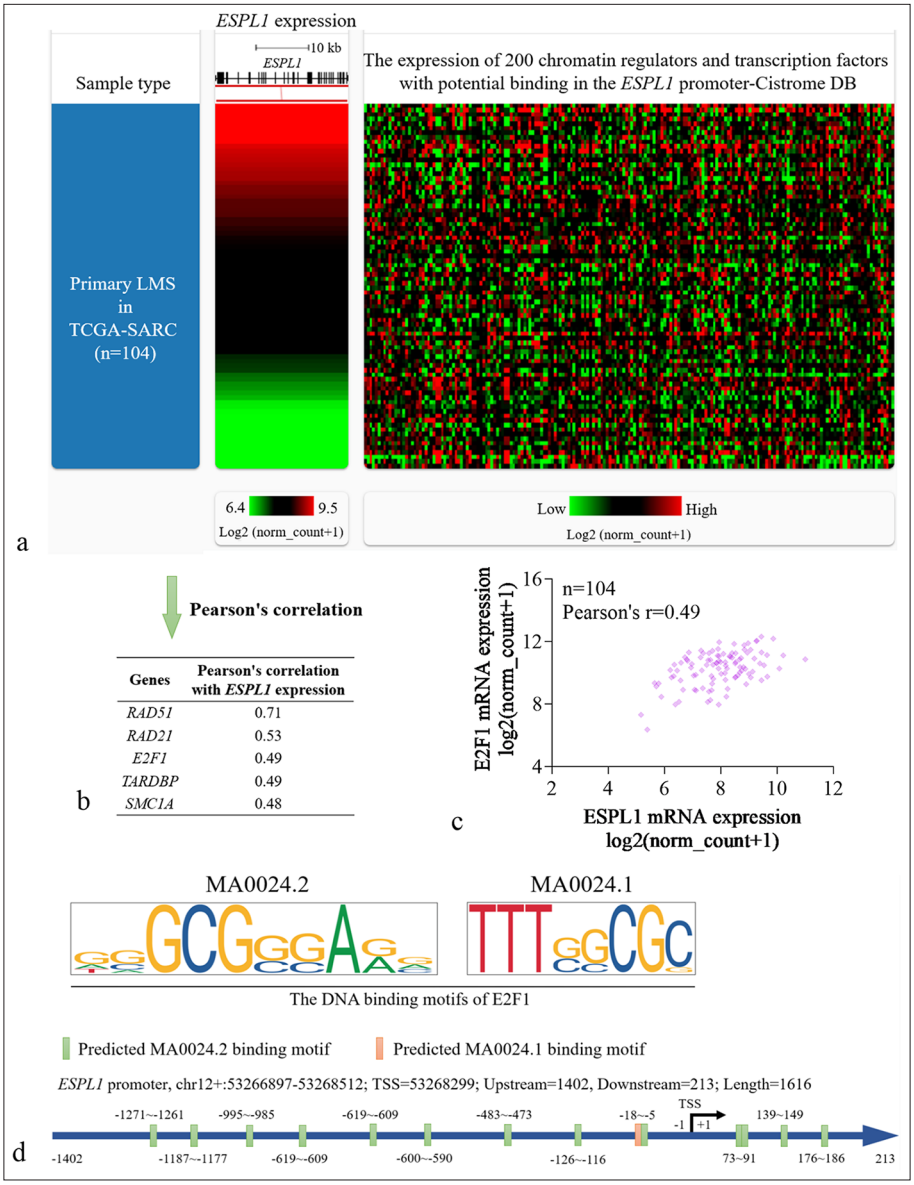

Figure 3: Bioinformatics analysis identified E2F1 as a transcription factor with potential regulatory effects on *ESPL1* expression in LMS. (a) Heatmap showing the expression correlation of *ESPL1* (left) and 200 chromatin regulators and transcription factors with potential binding to the *ESPL1* promoter (right) (within 1 kb of the TSS site) in primary LMS cases from the TCGA-SARC dataset (*n*=104). (b) Table listing the top transcription factors and chromatin regulators with significant Pearson correlation coefficients with *ESPL1* expression in LMS patients. (c) Scatter plot depicting the correlation between *ESPL1* and *E2F1* expression in LMS patients, with a Pearson correlation coefficient of 0.49 (*n*=104). (d) Visualization of E2F1 binding motifs (MA0024.2 and MA0024.1) predicted in the *ESPL1* promoter region. Binding motifs are indicated with green and pink bars showing the predicted locations of the MA0024.2 and MA0024.1 binding sites, respectively. ESPL1: Extra spindle pole bodies like 1, LMS: Leiomyosarcoma, TCGA-SARC: The cancer genome atlas sarcoma, TSS: Transcription start site.

LMS compared with normal muscle tissues and that higher *ESPL1* expression is associated with poorer PFI and OS in sarcoma patients, especially in the LMS subset. In addition, univariate and multivariate analyses confirmed that *ESPL1* expression is an independent prognostic factor for poor OS (HR = 1.837; 95% CI: 1.249–2.704; *P* = 0.002) and PFI

Table 4: The predicted high-score binding sites of E2F1 in the promoter region of *ESPL1*.

Matrix ID	Score	Relative score	Sequence ID	Start	End	Strand	Predicted sequence
MA0024.2	8.54	0.90	HPRM47346	1476	1486	+	GGGGCGGTAAG
MA0024.2	6.92	0.87	HPRM47346	1277	1287	+	GCCGCGGGAGC
MA0024.1	8.83	0.87	HPRM47346	1385	1392	+	TCTGGCGC
MA0024.2	6.79	0.87	HPRM47346	216	226	+	GTGGCGGGATC
MA0024.2	6.72	0.87	HPRM47346	920	930	+	GAGGTGGGAGG
MA0024.2	6.69	0.87	HPRM47346	1388	1398	+	GGCGCGGAAAA
MA0024.2	6.69	0.87	HPRM47346	1579	1589	+	GTGTCGGGAGG
MA0024.2	6.61	0.87	HPRM47346	132	142	+	CAGGCGTGAGC
MA0024.2	6.49	0.87	HPRM47346	784	794	+	AAGGCTGGAAG
MA0024.2	6.49	0.87	HPRM47346	1484	1494	+	AAGGCCGGAAG
MA0024.2	6.01	0.86	HPRM47346	803	813	+	AGAGCTGGAGG
MA0024.2	5.99	0.86	HPRM47346	408	418	+	TAGGCGTGAGC
MA0024.2	5.78	0.85	HPRM47346	1542	1552	+	CTGACGCGAGG
MA0024.2	5.49	0.85	HPRM47346	1292	1302	+	AGCGCGGCGGG

(HR = 1.683; 95% CI: 1.270–2.231; $P < 0.001$) in LMS patients. This finding is consistent with previous studies showing that aberrant expression of *ESPL1* is correlated with poor survival outcomes in hepatocellular carcinoma (HCC),[17] gastric cancer,[18] bladder cancer,[19] and glioma.[20] Recent studies have shown that elevated serum ESPL1 levels may indicate hepatitis B virus (HBV) S gene integration and a greater risk of HBV-related HCC, making it a promising biomarker for screening high-risk populations and monitoring recurrence in HBV-related HCC patients.[21,22] In future, we will explore the potential of serum ESPL1 as a biomarker in patients with LMS.

PARADIGM pathway analysis in LMS patients further revealed that increased *ESPL1* expression is strongly associated with increased activity in pathways related to mitotic processes, transcription factor networks, and chromatid cohesion, underscoring the importance of ESPL1 in the regulation of the cell cycle and genomic integrity in LMS. These findings imply that ESPL1 may play a critical role in the aggressive behavior of this sarcoma subtype. Our functional studies revealed that the knockdown of *ESPL1* significantly impaired cell proliferation and clonogenic capacity, suggesting that ESPL1 is crucial for maintaining the viability and growth of LMS cells. Importantly, the profound G2/M cell cycle arrest induced by ESPL1 silencing highlights its specific regulatory function in LMS, reinforcing its potential as a therapeutic target. These findings are consistent with the well-established role of ESPL1 in controlling sister chromatid separation during mitosis.[23,24]

Although *ESPL1* overexpression is observed in multiple types of cancer,[17-20] the genetic or epigenetic alterations leading to its dysregulation are still unclear. To understand the transcriptional regulation of *ESPL1* in LMS, we employed a comprehensive bioinformatics approach to identify potential transcriptional regulators. Our analysis highlighted E2F1 as a key transcription factor that is positively correlated with ESPL1 expression in LMS samples and may directly bind to the *ESPL1* promoter region. E2F1 plays pivotal roles in regulating genes that control the cell cycle, DNA replication, and chromosomal stability.[25] Its overexpression, together with the upregulation of FOXM1 and WEE1, can drive the development of soft tissue sarcoma.[26]

The significant overexpression of *E2F1* in LMS samples, together with the observation that *E2F1* knockdown leads to a concomitant reduction in *ESPL1* expression and promoter activity, strongly suggest that E2F1 transcriptionally activates ESPL1 in LMS. Mechanistically, ChIP-qPCR analysis confirmed the direct binding of E2F1 to the *ESPL1* promoter region, and a dual-luciferase assay confirmed the transcriptional activation effects of E2F1 on the *ESPL1* promoter. These findings align with previous reports demonstrating that E2F1 can transcriptionally regulate genes associated with sister chromatid cohesion and separation.[27,28] The identification of E2F1 as a key transcriptional regulator of ESPL1 in LMS further highlights the intricate interplay between cell cycle control, genomic stability, and sarcoma pathogenesis.

The overexpression of ESPL1 and its association with poor survival outcomes in sarcoma patients, particularly in the LMS subset, suggest that ESPL1 may serve as a potential prognostic biomarker and therapeutic target in these malignancies. Inhibiting ESPL1 function or disrupting its transcriptional regulation by E2F1 could be a promising strategy to suppress the proliferation and genomic instability of LMS cells.

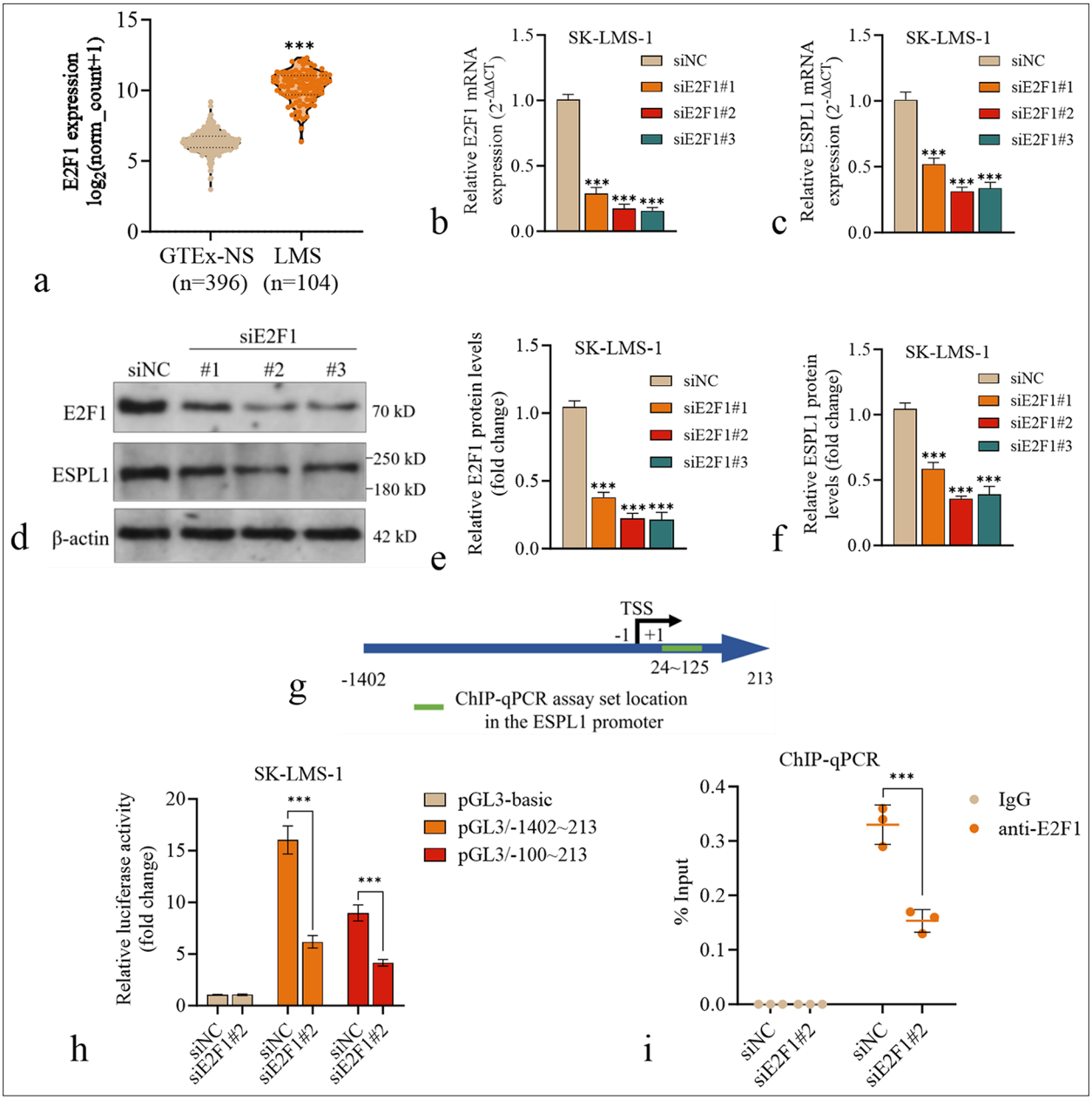

Figure 4: Validation of the effects of E2F1 transcriptional activation on the ESPL1 promoter in LMS. (a) Violin plot comparing *ESPL1* expression between normal muscle tissues from the GTEx dataset (GTEx-NS, *n*=396) and primary LMS tissues from the TCGA-SARC dataset (*n*=104). (b and c) The relative mRNA expression of *E2F1* (b) and *ESPL1* (c) in SK-LMS-1 cells 24 h after transfection with siNC or siE2F1 (#1, #2, #3). (d-f) Western blotting images (d) and quantification (e and f) of E2F1 and ESPL1 protein levels in SK-LMS-1 cells 24 h after transfection with siNC or siE2F1 (#1, #2, #3). (g) A schematic diagram illustrating the *ESPL1* promoter region and the location of the targeting region in the ChIP-qPCR assay. (h) Luciferase reporter assay to measure the transcriptional activity of the *ESPL1* promoter in SK-LMS-1 cells. The cells were cotransfected with siNC or siE2F1 (#2) and luciferase reporter constructs containing either the full *ESPL1* promoter region (−1402 to +213) or the truncated promoter region (−100 to +213). The data are presented as the fold change in relative luciferase activity normalized to that of siNC. (i) ChIP-qPCR analysis of E2F1 binding to the *ESPL1* promoter in SK-LMS-1 cells with or without *E2F1* knockdown. IgG was used as a negative control. The enrichment of E2F1 binding is shown as the % input. ***P<0.001. ESPL1: Extra spindle pole bodies like 1, ChIP: Chromatin Immunoprecipitation, GTEx: Genotype-tissue expression, LMS: Leiomyosarcoma, OS: Overall survival, IgG: Immunoglobulin G, qPCR: Quantitative polymerase chain reaction.

Since E2F1 directly regulates *ESPL1* expression, small molecules or RNA-based therapies (e.g., RNA interference or CRISPR/Cas9-mediated knockdown) that disrupt the E2F1-ESPL1 interaction could selectively reduce ESPL1

expression in LMS cells. This approach may be more specific than targeting ESPL1 alone, reducing the potential for off-target effects. Inhibiting both ESPL1 and E2F1, or combining this strategy with other treatments targeting cell cycle checkpoints or mitotic regulators (e.g., WEE1 inhibitors), could enhance therapeutic efficacy. Given the role of ESPL1 and E2F1 in cell cycle progression, combining these therapies with chemotherapy or radiation could potentiate their effects by inducing synthetic lethality.

A limitation of our study is the reliance on a single cell line, SK-LMS-1, for functional experiments. While SK-LMS-1 is a well-established model for LMS, we acknowledge that it may not fully represent the heterogeneity observed in LMS tumors. LMS is known for its diverse molecular and genetic profiles, which can vary depending on the anatomical site of origin and other factors.[3] Therefore, the results obtained from SK-LMS-1 cells may not be universally applicable to all LMS subtypes or patient-derived tumors. To address this limitation and validate our findings across a broader spectrum of LMS, future studies should incorporate primary patient-derived LMS cells or patient-derived organoids. This approach could provide valuable insights into the role of ESPL1 in a more physiologically relevant setting that better recapitulates the tumor microenvironment.

SUMMARY

In conclusion, our study identified *ESPL1* as a potential prognostic biomarker in LMS, as its overexpression is strongly associated with poor survival outcomes. We demonstrated that ESPL1 plays a crucial role in LMS cell proliferation and cell cycle progression, particularly at the G2/M phase. Furthermore, we elucidated the underlying mechanism of *ESPL1* upregulation in LMS by identifying E2F1 as a key transcriptional regulator.

AVAILABILITY OF DATA AND MATERIALS

The datasets generated and analyzed during the current study are available from the corresponding author on reasonable request. Public data used in this study can be accessed through the TCGA-SARC and GTEx databases.

ABBREVIATIONS

ATCC: American Type Culture Collection
CCK-8: Cell Counting Kit-8
ChIP: Chromatin Immunoprecipitation
DDLS: Dedifferentiated Liposarcoma
ESPL1: Extra Spindle Pole Bodies Like 1
GTEx: Genotype-Tissue Expression
HPA: Human Protein Atlas
IHC: Immunohistochemistry
LMS: Leiomyosarcoma
MFS: Myxofibrosarcoma
MPNST: Malignant Peripheral Nerve Sheath Tumors
OS: Overall Survival
PFI: Progression-Free Interval
PI: Propidium Iodide
qRT-PCR: Quantitative Real-Time PCR
siRNA: Small Interfering RNA
SS: Synovial Sarcoma
TCGA-SARC: The Cancer Genome Atlas Sarcoma
TSS: Transcription Start Site
UPS: Undifferentiated Pleomorphic Sarcoma

AUTHOR CONTRIBUTIONS

XY, GM, and GT: Conceived and designed the study; XY, QW, and QY: Performed the experiments and analyzed the data; QH: Provided clinical insights and interpretation; XY and GT: Wrote the manuscript. All authors reviewed and approved the final version of the manuscript.

ETHICS APPROVAL AND CONSENT TO PARTICIPATE

Institutional Review Board approval is not required as this study did not involve human or anuman experiments. Patient consent not required as there are no patients in this study.

ACKNOWLEDGMENT

This study was supported by Sichuan Medical Association Orthopedics (Shang Antong) special research topic (2023SAT02).

FUNDING

Not applicable.

CONFLICT OF INTEREST

The authors declare no conflict of interest.

EDITORIAL/PEER REVIEW

To ensure the integrity and highest quality of CytoJournal publications, the review process of this manuscript was conducted under a **double-blind model** (authors are blinded for reviewers and vice versa) through an automatic online system.

REFERENCES

1. Cancer Genome Atlas Research Network. Comprehensive and integrated genomic characterization of adult soft tissue sarcomas. Cell 2017;171:950-65.e28.
2. Menon G, Mangla A, Yadav U. Leiomyosarcoma. In: StatPearls. Treasure Island, FL: StatPearls Publishing; 2024.
3. Kerrison WG, Thway K, Jones RL, Huang PH. The biology and treatment of leiomyosarcomas. Crit Rev Oncol Hematol

2023;184:103955.
4. Li PH, Kong XY, He YZ, Liu Y, Peng X, Li ZH, *et al.* Recent developments in application of single-cell RNA sequencing in the tumour immune microenvironment and cancer therapy. Mil Med Res 2022;9:52.
5. Seligson ND, Tang J, Jin DX, Bennett MP, Elvin JA, Graim K, *et al.* Drivers of genomic loss of heterozygosity in leiomyosarcoma are distinct from carcinomas. NPJ Precis Oncol 2022;6:29.
6. Wolf PG, Cuba Ramos A, Kenzel J, Neumann B, Stemmann O. Studying meiotic cohesin in somatic cells reveals that Rec8-containing cohesin requires Stag3 to function and is regulated by Wapl and sororin. J Cell Sci 2018;131:jcs212100.
7. Försti A, Frank C, Smolkova B, Kazimirova A, Barancokova M, Vymetalkova V, *et al.* Genetic variation in the major mitotic checkpoint genes associated with chromosomal aberrations in healthy humans. Cancer Lett 2016;380:442-6.
8. Kulus J, Kranc W, Kulus M, Dzięgiel P, Bukowska D, Mozdziak P, *et al.* Expression of genes regulating cell division in porcine follicular granulosa cells. Cell Div 2023;18:12.
9. Prinzhorn W, Stehle M, Kleiner H, Ruppenthal S, Müller MC, Hofmann WK, *et al.* c-MYB is a transcriptional regulator of ESPL1/Separase in BCR-ABL-positive chronic myeloid leukemia. Biomark Res 2016;4:5.
10. Zhang W, Wang Y, Tang Q, Li Z, Sun J, Zhao Z, *et al.* PAX2 mediated upregulation of ESPL1 contributes to cisplatin resistance in bladder cancer through activating the JAK2/STAT3 pathway. Naunyn Schmiedebergs Arch Pharmacol 2024;397:6889-901.
11. Goldman MJ, Craft B, Hastie M, Repečka K, McDade F, Kamath A, *et al.* Visualizing and interpreting cancer genomics data via the Xena platform. Nat Biotechnol 2020;38:675-8.
12. Uhlen M, Zhang C, Lee S, Sjöstedt E, Fagerberg L, Bidkhori G, *et al.* A pathology atlas of the human cancer transcriptome. Science 2017;357:eaan2507.
13. Zheng R, Wan C, Mei S, Qin Q, Wu Q, Sun H, *et al.* Cistrome data browser: Expanded datasets and new tools for gene regulatory analysis. Nucleic Acids Res 2019;47:D729-35.
14. Wassing IE, Graham E, Saayman X, Rampazzo L, Ralf C, Bassett A, *et al.* The RAD51 recombinase protects mitotic chromatin in human cells. Nat Commun 2021;12:5380.
15. Huber K, Giralt A, Dreos R, Michenthaler H, Geller S, Barquissau V, *et al.* E2F transcription factor-1 modulates expression of glutamine metabolic genes in mouse embryonic fibroblasts and uterine sarcoma cells. Biochim Biophys Acta Mol Cell Res 2024;1871:119721.
16. Rauluseviciute I, Riudavets-Puig R, Blanc-Mathieu R, Castro-Mondragon JA, Ferenc K, Kumar V, *et al.* JASPAR 2024: 20th anniversary of the open-access database of transcription factor binding profiles. Nucleic Acids Res 2024;52 D174-82.
17. Song R, Huang J, Yang C, Li Y, Zhan G, Xiang B. ESPL1 is elevated in hepatocellular carcinoma and predicts prognosis. Int J Gen Med 2022;15:8381-98.
18. Zhang B, Chen Y, Chen X, Ren Z, Xiang H, Mao L, *et al.* Genome-wide CRISPR screen identifies ESPL1 limits the response of gastric cancer cells to apatinib. Cancer Cell Int 2024;24:83.
19. Zhang W, Liang ZQ, He RQ, Huang ZG, Wang XM, Wei MY, *et al.* The upregulation and transcriptional regulatory mechanisms of Extra spindle pole bodies like 1 in bladder cancer: An immunohistochemistry and high-throughput screening Evaluation. Heliyon 2024;10:e31192.
20. Liu Z, Lian X, Zhang X, Zhu Y, Zhang W, Wang J, *et al.* ESPL1 Is a novel prognostic biomarker associated with the malignant features of glioma. Front Genet 2021;12:666106.
21. Wang R, Zang W, Hu B, Deng D, Ling X, Zhou H, *et al.* Serum ESPL1 can be used as a biomarker for patients with hepatitis B virus-related liver cancer: A Chinese case-control study. Technol Cancer Res Treat 2020;19:1533033820980785.
22. Hu B, Wei LU, Liang H, Su M, Wang R, Su T, *et al.* Correlation between serum ESPL1 and hepatitis B virus-related hepatocellular carcinoma histological grade: A Chinese single-center case-control study. Anticancer Res 2023;43:3997-4005.
23. Zhong Y, Zheng C, Zhang W, Wu H, Wang M, Zhang Q, *et al.* Pan-cancer analysis and experimental validation identify the oncogenic nature of ESPL1: Potential therapeutic target in colorectal cancer. Front Immunol 2023;14:1138077.
24. Koedoot E, van Steijn E, Vermeer M, González-Prieto R, Vertegaal AC, Martens JW, *et al.* Splicing factors control triple-negative breast cancer cell mitosis through SUN2 interaction and sororin intron retention. J Exp Clin Cancer Res 2021;40:82.
25. Lu Y, Wei Y, Shen X, Tong Y, Lu J, Zhang Y, *et al.* Mechanism of E2F1 in the proliferation, migration, and invasion of endometrial carcinoma cells via the regulation of BMI1 transcription. Genes Genomics 2023;45:1423-31.
26. Ke XY, Chen Y, Tham VY, Lin RY, Dakle P, Nacro K, *et al.* MNK1 and MNK2 enforce expression of E2F1, FOXM1, and WEE1 to drive soft tissue sarcoma. Oncogene 2021;40:1851-67.
27. Wen J, Wang X, Yang G, Zheng J. AURKA promotes renal cell carcinoma progression via regulation of CCNB1 transcription. Heliyon 2024;10:e27959.
28. Rotelli MD, Policastro RA, Bolling AM, Killion AW, Weinberg AJ, Dixon MJ, *et al.* A Cyclin A-Myb-MuvB-Aurora B network regulates the choice between mitotic cycles and polyploid endoreplication cycles. PLoS Genet 2019;15:e1008253.

How to cite this article: Yang X, Miao G, Wang Q, Yu Q, Hu Q, Tan G. E2F1-mediated *ESPL1* transcriptional activation predicts poor prognosis and promotes the proliferation of leiomyosarcoma. CytoJournal. 2025;22:3. doi: 10.25259/Cytojournal_178_2024

HTML of this article is available FREE at:
https://dx.doi.org/10.25259/Cytojournal_178_2024